CEA-R-6235

ISSN 0429 - 3460

COMMISSARIAT À L'ÉNERGIE ATOMIQUE

DIRECTION DE LA RECHERCHE TECHNOLOGIQUE

CONVERSION COEFFICIENTS FROM AIR KERMA TO PERSONNAL DOSE EQUIVALENT $H_p(3)$ FOR EYE-LENS DOSIMETRY

par

Josiane DAURES, Jean GOURIOU, Jean-Marc BORDY

CEA SACLAY
DIRECTION DE LA RECHERCHE TECHNOLOGIQUE
LABORATOIRE D'INTÉGRATION DES SYSTÈMES ET DES TECHNOLOGIES
DÉPARTEMENT DES TECHNOLOGIES DU CAPTEUR ET DU SIGNAL
LABORATOIRE NATIONAL HENRI BECQUEREL

RAPPORT

DIRECTION DES SYSTÈMES D'INFORMATION

CEA / SACLAY 91191 GIF-SUR-YVETTE CEDEX FRANCE

2009

RAPPORT CEA-R-6235

RAPPORT CEA-R-6235 – Josiane DAURES, Jean GOURIOU, Jean-Marc BORDY

«Coefficients de conversion du kerma dans l'air à l'équivalent de dose individuel $H_p(3)$ pour la dosimétrie du cristallin»

Résumé - Ce travail a été effectué dans le cadre du projet ORAMED (Optimization of RAdiation protection for MEDical staff) de l'Union Européenne. L'objet principal de ce projet est d'améliorer les standards de protection du personnel médical pour les procédures pouvant conduire à des expositions potentiellement élevées et de développer des méthodologies pour une meilleure estimation et une réduction de l'exposition. Le groupe de travail WP2 est en charge du développement d'une dosimétrie du cristallin dans la pratique en radiologie interventionnelle. Cette étude est complémentaire de la partie du rapport de l'ENEA concernant le calcul des coefficients de conversion liés à la grandeur opérationnelle $H_p(3)$. Un ensemble de coefficients de conversion $H_p(3)/K_{air}$, en fonction de l'énergie et de l'angle, dans le nouveau fantôme proposé constitué d'un cylindrique droit en matériau tissu quatre éléments, ont été calculés à l'aide du code de Monte-Carlo PENELOPE. Les valeurs de $H_p(3)$ ont été déterminées en termes de dose absorbée, conformément à la définition de cette grandeur, ainsi qu'en utilisant l'approximation kerma précédemment reportée dans les rapports de l'ICRU. Pour les photons de faible énergie, jusqu'à 1 MeV, les deux séries de facteurs de conversions sont en bon accord. Néanmoins, les différences augmentent à plus haute énergies. Ceci est principalement du au manque d'équilibre électronique, particulièrement pour les faibles angles d'incidence. Les valeurs des coefficients de conversion obtenues avec le code MCNP publiées par l'ENEA sont en accord avec les calculs PENELOPE selon l'approximation kerma. Ils sont cohérents avec des calculs antérieurs dans des fantômes de géométries différentes. Cependant, à partir de 1 MeV les différences entre les facteurs de conversion calculés en termes de dose absorbée ou avec l'approximation kerma augmentent significativement, particulièrement pour les faibles angles d'incidence. A ces énergies le transport des électrons doit être simulé.

Mots Clés : Equivalent de dose individuel; dosimétrie du cristallin; coefficients de conversion; PENELOPE code; simulations Mont-Carlo; grandeurs opérationnelles.

2009 - Commissariat à l'Énergie Atomique – France

RAPPORT CEA-R-6235 – Josiane DAURES, Jean GOURIOU, Jean-Marc BORDY

«Conversion coefficients from air kerma to personal dose equivalent $H_p(3)$ for eye-lens dosimetry)»

Abstract - This work has been performed within the frame of the European Union ORAMED project (Optimization of RAdiation protection for MEDical staff). The main goal of the project is to improve standards of protection for medical staff for procedure resulting in potentially high exposures and to develop methodologies for better assessing and for reducing exposures to medical staff. The Work Package WP2 is involved in the development of practical eye lens dosimetry in interventional radiology. This study is complementary of the part of the ENEA report concerning the calculations with the MCNP code of the conversion factors related to the operational quantity $H_p(3)$. A set of energy and angular dependent conversion coefficients $H_p(3)/K_{air}$ in the new proposed square cylindrical phantom of ICRU tissue, have been calculated with the Monte-Carlo code PENELOPE. The $H_p(3)$ values have been determined in terms of absorbed dose, according to the definition of this quantity, and also with the kerma approximation as formerly reported in ICRU reports. At low photon energy, up to 1 MeV, the two sets of conversion coefficients are consistent. Nevertheless, the differences increase at higher energy. This is mainly due to the lack of electronic equilibrium, especially for small angle incidences. The values of the conversion coefficients obtained with the code MCNP published by ENEA, agree with the kerma approximation calculations with PENELOPE. They are coherent with previous calculations in phantoms different in shape. But above 1 MeV, differences between conversion coefficient values calculated with the absorbed dose and with kerma approximation are significantly increasing, especially at low incidence angles. At those energies the electron transport has to be simulated.

Key Words: Personal dose equivalent, eye-lens dosimetry; conversion coefficients; PENELOPE code; Mont-Carlo simulations; operational quantities

2009 – Commissariat à l'Énergie Atomique – France

- Rapport CEA-R-6235 -

CEA Saclay
Direction de la Recherche Technologique
Laboratoire d'Intégration des Systèmes et des Technologies
Département des Technologies du Capteur et du Signal
Laboratoire National Henri Becquerel

CONVERSION COEFFICIENTS FROM AIR KERMA TO PERSONNAL DOSE EQUIVALENT $H_p(3)$ FOR EYE-LENS DOSIMETRY

Par

Josiane DAURES, Jean GOURIOU,
Jean-Marc BORDY

- Décembre 2009 -

Conversion coefficients from air kerma to personal dose equivalent $H_p(3)$ for eye-lens dosimetry

ORAMED project

Rapport CEA

J. Daures[1], J. Gouriou[1], JM Bordy[1]

[1]CEA, LIST, Laboratoire National Henri Becquerel (LNE LNHB), F-91191 Gif-sur-Yvette, France.

Summary

This work has been performed within the frame of the European Union ORAMED project (Optimization of RAdiation protection for MEDical staff). The main goal of the project is to improve standards of protection for medical staff for procedure resulting in potentially high exposures and to develop methodologies for better assessing and for reducing exposures to medical staff.

The Work Package WP2 is involved in the development of practical eye lens dosimetry in interventional radiology. This study is complementary of the part of the ENEA report concerning the calculations with the MCNP code of the conversion factors related to the operational quantity $H_p(3)$.

A set of energy and angular dependent conversion coefficients $H_p(3)/K_{air}$ in the new proposed square cylindrical phantom of ICRU tissue, have been calculated with the Monte-Carlo code PENELOPE. The $H_p(3)$ values have been determined in terms of absorbed dose, according to the definition of this quantity, and also with the kerma approximation as formerly reported in ICRU reports. At low photon energy, up to 1 MeV, the two sets of conversion coefficients are consistent. Nevertheless, the differences increase at higher energy. This is mainly due to the lack of electronic equilibrium, especially for small angle incidences.

The values of the conversion coefficients obtained with the code MCNP published by ENEA, agree with the kerma approximation calculations with PENELOPE. They are coherent with previous calculations in phantoms different in shape.

But above 1 MeV, differences between conversion coefficient values calculated with the absorbed dose and with kerma approximation are significantly increasing, especially at low incidence angles. At those energies the electron transport has to be simulated.

Key Words **:** Personal dose equivalent*,* eye-lens dosimetry; conversion coefficients; PENELOPE code; Mont-Carlo simulations; operational quantities

Coefficients de conversion du kerma dans l'air à l'équivalent de dose individuel $H_p(3)$ pour la dosimétrie du cristallin

ORAMED project

Rapport CEA

J. Daures(1), J. Gouriou(1), JM Bordy(1)

(1)CEA, LIST, Laboratoire National Henri Becquerel (LNE LNHB), F-91191 Gif-sur-Yvette, France.

Résumé

Ce travail a été effectué dans le cadre du projet ORAMED (Optimization of RAdiation protection for MEDical staff) de l'Union Européenne. L'objet principal de ce projet est d'améliorer les standards de protection du personnel médical pour les procédures pouvant conduire à des expositions potentiellement élevées et de développer des méthodologies pour une meilleure estimation et une réduction de l'exposition.

Le groupe de travail WP2 est en charge du développement d'une dosimétrie du cristallin dans la pratique en radiologie interventionnelle. Cette étude est complémentaire de la partie du rapport de l'ENEA concernant le calcul des coefficients de conversion liés à la grandeur opérationnelle $H_p(3)$.

Un ensemble de coefficients de conversion $H_p(3)/K_{air}$, en fonction de l'énergie et de l'angle, dans le nouveau fantôme proposé constitué d'un cylindrique droit en matériau tissu quatre éléments, ont été calculés à l'aide du code de Monte-Carlo PENELOPE. Les valeurs de $H_p(3)$ ont été déterminées en termes de dose absorbée, conformément à la définition de cette grandeur, ainsi qu'en utilisant l'approximation kerma précédemment reportée dans les rapports de l'ICRU. Pour les photons de faible énergie, jusqu'à 1 MeV, les deux séries de facteurs de conversions sont en bon accord. Néanmoins, les différences augmentent à plus haute énergies. Ceci est principalement du au manque d'équilibre électronique, particulièrement pour les faibles angles d'incidence.

Les valeurs des coefficients de conversion obtenues avec le code MCNP publiées par l'ENEA sont en accord avec les calculs PENELOPE selon l'approximation kerma. Ils sont cohérents avec des calculs antérieurs dans des fantômes de géométries différentes.

Cependant, à partir de 1 MeV les différences entre les facteurs de conversion calculés en termes de dose absorbée ou avec l'approximation kerma augmentent significativement, particulièrement pour les faibles angles d'incidence. A ces énergies le transport des électrons doit être simulé.

***Mots Clés* :** Equivalent de dose individuel; dosimétrie du cristallin; coefficients de conversion; PENELOPE code; simulations Mont-Carlo; grandeurs opérationnelles.

The present study is supported by the ORAMED Contract (FP7 Grant Agreement 211361 started on February 1st 2008).

CEA SACLAY
DIRECTION DE LA RECHERCHE TECHNOLOGIQUE
LABORATOIRE D'INTEGRATION DES SYSTEMES ET DES TECHNOLOGIES
DEPARTEMENT DES TECHNOLOGIES DU CAPTEUR ET DU SIGNAL
LABORATOIRE NATIONAL HENRI BECQUEREL

CONTENTS

1 Introduction

This work has been performed within the frame of the European Union ORAMED project (Optimization of RAdiation protection for MEDical staff) [1]. The main goal of the project is to improve standards of protection for medical staff for procedure resulting in potentially high exposures and develop methodologies for better assessing and reducing exposures to medical staff.

The Work Package WP2 is involved in the development of practical eye lens dosimetry in interventional radiology. This study is complementary of the part of the ENEA report [2] concerning the calculations of the conversion factors.

The design of a phantom well suited for eye-lens dosimetry has been discussed within WP2. It appears that a right cylinder, 20 cm in diameter and 20 cm height, is more appropriate than the 30 cm x 30 cm x 15 cm ISO slab phantom or even the reduced slab phantom (20 cm x 20 cm x 15 cm). This new phantom constituted of ICRU four elements is used to calculate the personal dose equivalent $H_p(3)$ and the conversion coefficient $H_p(3)/K_{air}$. These values of the conversion coefficient $H_p(3)/K_{air}$ will be very helpful because ICRU 57 [3] do not provide tabulated values for the depth of 3 mm for photons.

Similar phantom in shape, a cylinder of PMMA having a wall of 1 cm, filled with water will be then used to perform the calibration of the personal dosimeters.

In this study a set of energy and angular dependent conversion coefficient $H_p(3)/K_{air}$ in the new proposed right cylindrical phantom made of ICRU tissue have been calculated with the Monte-Carlo code PENELOPE [4]. The $H_p(3)$ values are calculated in terms of absorbed dose, according to the ICRU definition of this quantity [5] [6], together with the kerma approximation as formerly used. The K_{air} values have been also calculated with PENELOPE for global coherence.

The results of this work are compared with similar simulations performed at ENEA [2] with the code MCNP. It is important to have several independent determinations of the conversion coefficients.

2 Materials and methods

The simulations have been carried out with the Monte-Carlo code PENELOPE parallelised at CEA-LIST [7] on the LNHB cluster constituted of 112 processors (2.8 MHz).

The $H_p(3)/K_{air}$ conversion factor calculation implies the simulation of $H_p(3)$ and K_{air}.

Both quantities refer to unit fluence, but for a sake of simplicity, $H_p(3)/\Phi$ is written $H_p(3)$ and K_{air}/Φ is written K_{air}

2.1 Hp(3) calculations

The personal dose equivalent $H_p(3)$ is defined as the dose equivalent in tissue at 3 mm depth in the phantom. As it is recommended to take the quality factor Q equal to 1 for photons [8,9], $H_p(3)$ is equal to the absorbed dose in these specified conditions.

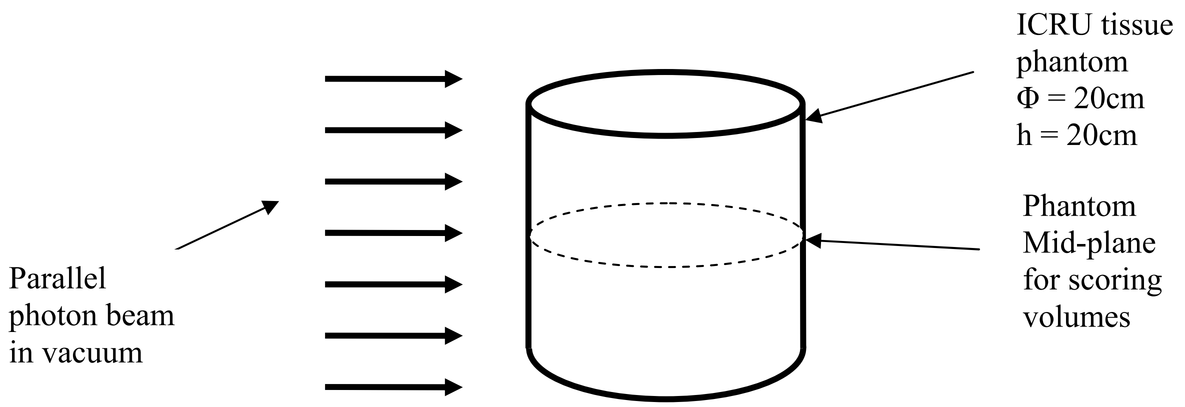

Figure 1 : Scheme of the geometry for $H_p(3)$ simulations.

The scheme of the geometry is given in the figure 1. The phantom is a right cylinder of 20 cm in diameter and 20 cm height made of 4-element ICRU tissue with a mass density of 1 $g \cdot cm^{-3}$ and a weight composition of 76.2% oxygen, 11.1% carbon, 0.1% hydrogen and 2.6% nitrogen. The cylinder is entirely irradiated by a square parallel beam of 20 cm * 20 cm. The simulations have been performed for monoenergetic photons from 20 keV up to 10 MeV as agreed with ENEA [2] in theses specific conditions and in ICRU 57 [3] for the $H_p(0.07)/K_{air}$ and $H_p(10)/K_{air}$ in the slab ICRU phantom (30 cm * 30 cm * 15 cm).

Due to the cylindrical geometry, the angular coefficients have been calculated in the same run. The scoring volumes have been positioned every 15 degrees.

The centers of the scoring volumes are positioned on the mid plane at the depth of 3 mm. The thickness is 0.5 mm along the radius, the height is 5 cm and the angle 0.4 degree (corresponding to a width of is 1 mm).

The output screen of the geometry defined in PENELOPE on the phantom mid plane is given in figure 2.

The behaviour of the secondary particles electrons and positrons in PENELOPE, is governed by the absorption energy parameters Eabs(1) and Eabs(3) respectively, which are the energies where particles are assumed to be effectively stopped and absorbed in the medium.

The interesting output value from PENELOPE is the average deposited energy in the scoring volume. This quantity expressed in joule, divided by the mass corresponding to the scoring volume expressed in kg leads to the kerma or absorbed dose depending on the parameters used for the transport of the charged particles.

- If Eabs(1) and Eabs(3) are greater than the most energetic secondary particles, all the energy transferred to the secondary charged particles is absorbed in the medium at the point of interaction, matching the kerma definition. This represents the kerma-approximation.
- If Eabs(1) and Eabs(3) are low, for example 1 or 10 keV, then the charged particles are carefully followed until they stop which characterize the energy imparted to the to the matter, corresponding to the absorbed dose definition.

$H_p(3)$ has been calculated both way, in terms of kerma and in terms of absorbed dose.

The results are given in section 3.

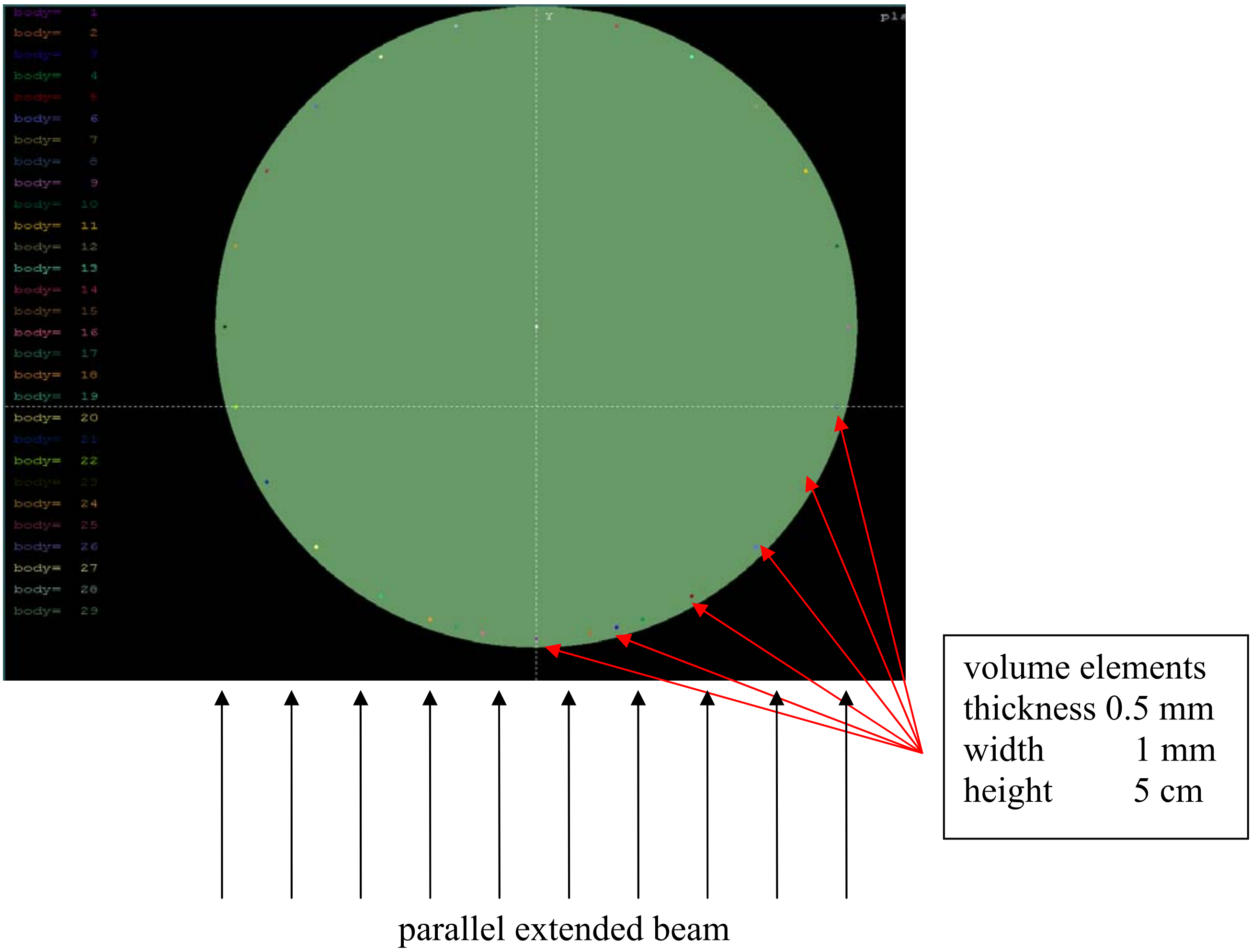

Figure 2 : Output screen of the geometry for $H_p(3)$ simulations

2.2 K_{air} calculations

The values of air kerma per unit fluence have been given in ICRU report 57 [3]. It can also be calculated from the mass energy-transfer coefficient $(\mu_{tr}/\rho)_{air}$ determined from Hubbell [10] by applying the following equation :

$$K_{air} / \Phi = E \cdot (\mu_{tr} / \rho)_{air}$$

Nevertheless, for a better consistency of the ratio $H_p(3)/K_{air}$, calculations have been performed with PENELOPE using the same set of cross sections. The parameters Eabs(1) and Eabs(3) are greater than the most energetic secondary particles to match the kerma definition.

The results are given in section 3.

3 Results

3.1 K_{air} determination

K_{air} is first investigated because as the values of $H_p(3)$ are normalized to K_{air}. The values and the 1 σ type A estimated uncertainties calculated by PENELOPE are given in the table 1.

Table 1 : K_{air}/Φ values calculated with PENELOPE Monte-Carlo code from 20 keV to 10 MeV

Photon energy (keV)	Kair/Φ ($Gy{\cdot}cm^2$)	1 σ (%)
20	1.729E-12	0.04
30	7.400E-13	0.03
40	4.388E-13	0.10
50	3.288E-13	0.05
60	2.924E-13	0.12
70	2.912E-13	0.12
80	3.088E-13	0.11
90	3.375E-13	0.11
100	3.724E-13	0.10
110	4.120E-13	0.10
150	5.989E-13	0.04
200	8.541E-13	0.10
300	1.380E-12	0.05
500	2.380E-12	0.11
600	2.842E-12	0.05
700	3.284E-12	0.05
800	3.703E-12	0.06
900	4.098E-12	0.05
1000	4.473E-12	0.05
1100	4.839E-12	0.05
1500	6.137E-12	0.06
2000	7.547E-12	0.07
3000	9.952E-12	0.07
4000	1.211E-11	0.08
5000	1.414E-11	0.08
6000	1.613E-11	0.09
7000	1.810E-11	0.08
8000	2.008E-11	0.08
10000	2.405E-11	0.22

These values are consistent with the ICRU 57 values, except at low energy (20 to 60 keV) where the difference is between 1 and 2 %.

3.2 $H_p(3)/K_{air}$ conversion coefficients, with $H_p(3)$ calculated in terms of kerma approximation

The $H_p(3)/K_{air}$ conversion coefficients have been calculated for thirty energy values from 20 keV up to 10 MeV with the Monte-Carlo code PENELOPE with the kerma approximation. The values and the 1 σ type A estimated uncertainties are given in the table 3 to 12.

Table 2 : $H_p(3)/K_{air}$ conversion coefficient for 20, 30 and 40 keV for different incident angles calculated with PENELOPE in terms of kerma approximation.

Energy (keV)	**20**		**30**		**40**	
Angle	**Hp(3)/Kair**	**1σ**	**Hp(3)/Kair**	**1σ**	**Hp(3)/Kair**	**1σ**
degree	**Sv/Gy**	**%**	**Sv/Gy**	**%**	**Sv/Gy**	**%**
0	0.918	0.1	1.221	0.1	1.449	0.2
10	0.915	0.1	1.218	0.1	1.447	0.1
15	0.912	0.1	1.211	0.1	1.444	0.1
20	0.906	0.1	1.211	0.1	1.436	0.1
30	0.890	0.1	1.199	0.1	1.426	0.1
45	0.845	0.1	1.165	0.1	1.390	0.1
60	0.755	0.1	1.096	0.1	1.322	0.1
75	0.562	0.1	0.947	0.1	1.181	0.2
90	0.201	0.1	0.587	0.1	0.846	0.2
105	0.017	0.5	0.195	0.3	0.404	0.2
120	_	_	0.057	0.5	0.181	0.3
135	_	_	0.020	0.8	0.094	0.5
150	_	_	_	_	0.059	0.6
165	_	_	_	_	0.044	0.7
180	_	_	_	_	0.040	1.0

Table 3 : $H_p(3)/K_{air}$ conversion coefficient for 50, 60 and 70 keV for different incident angles calculated with PENELOPE in terms of kerma approximation.

Energy (keV)	**50**		**60**		**70**	
Angle	Hp(3)/Kair	1σ	Hp(3)/Kair	1σ	Hp(3)/Kair	1σ
degree	Sv/Gy	%	Sv/Gy	%	Sv/Gy	%
0.0	1.597	0.1	1.666	0.2	1.673	0.1
10.0	1.593	0.1	1.662	0.1	1.668	0.1
15.0	1.588	0.1	1.660	0.1	1.667	0.1
20.0	1.589	0.1	1.656	0.1	1.664	0.1
30.0	1.573	0.1	1.645	0.1	1.652	0.1
45.0	1.539	0.1	1.609	0.1	1.623	0.1
60.0	1.471	0.1	1.546	0.1	1.566	0.1
75.0	1.333	0.1	1.416	0.1	1.446	0.1
90.0	1.009	0.1	1.106	0.1	1.154	0.1
105.0	0.557	0.1	0.654	0.2	0.705	0.1
120.0	0.294	0.2	0.373	0.2	0.417	0.2
135.0	0.176	0.2	0.237	0.2	0.275	0.2
150.0	0.122	0.3	0.172	0.3	0.205	0.2
165.0	0.098	0.3	0.143	0.3	0.172	0.3
180.0	0.091	0.5	0.133	0.4	0.163	0.4

Table 4 : $H_p(3)/K_{air}$ conversion coefficient for 80, 90 and 100 keV for different incident angles calculated with PENELOPE in terms of kerma approximation.

Energy (keV)	**80**		**90**		**100**	
Angle	Hp(3)/Kair	1σ	Hp(3)/Kair	1σ	Hp(3)/Kair	1σ
degree	Sv/Gy	%	Sv/Gy	%	Sv/Gy	%
0	1.648	0.2	1.613	0.1	1.580	0.1
10	1.646	0.1	1.613	0.1	1.578	0.1
15	1.646	0.1	1.610	0.1	1.577	0.1
20	1.639	0.1	1.609	0.1	1.577	0.1
30	1.632	0.1	1.602	0.1	1.571	0.1
45	1.605	0.1	1.578	0.1	1.553	0.1
60	1.557	0.1	1.538	0.1	1.515	0.1
75	1.449	0.1	1.438	0.1	1.427	0.1
90	1.169	0.1	1.174	0.1	1.172	0.1
105	0.731	0.1	0.746	0.1	0.755	0.1
120	0.445	0.2	0.459	0.2	0.470	0.2
135	0.295	0.2	0.310	0.2	0.320	0.2
150	0.223	0.2	0.235	0.2	0.244	0.2
165	0.189	0.2	0.200	0.2	0.208	0.2
180	0.178	0.4	0.189	0.3	0.197	0.3

Table 5 : $H_p(3)/K_{air}$ conversion coefficient for 110, 150 and 200 keV for different incident angles calculated with PENELOPE in terms of kerma approximation.

Energy (keV)	**110**		**150**		**200**	
Angle	Hp(3)/Kair	1σ	Hp(3)/Kair	1σ	Hp(3)/Kair	1σ
degree	Sv/Gy	%	Sv/Gy	%	Sv/Gy	%
0	1.552	0.3	1.449	0.1	1.372	0.2
10	1.551	0.2	1.449	0.1	1.373	0.1
15	1.548	0.2	1.446	0.1	1.374	0.1
20	1.546	0.2	1.445	0.1	1.373	0.1
30	1.543	0.2	1.444	0.1	1.374	0.1
45	1.528	0.2	1.442	0.1	1.372	0.1
60	1.495	0.2	1.421	0.1	1.366	0.1
75	1.414	0.2	1.361	0.1	1.318	0.1
90	1.170	0.2	1.151	0.1	1.140	0.1
105	0.765	0.2	0.776	0.1	0.794	0.1
120	0.481	0.3	0.505	0.1	0.533	0.2
135	0.329	0.3	0.353	0.2	0.382	0.2
150	0.250	0.3	0.272	0.2	0.300	0.2
165	0.213	0.3	0.233	0.2	0.259	0.2
180	0.203	0.4	0.220	0.3	0.245	0.3

Table 6 : $H_p(3)/K_{air}$ conversion coefficient for 300, 400 and 500 keV for different incident angles calculated with PENELOPE in terms of kerma approximation.

Energy (keV)	**300**		**400**		**500**	
Angle	Hp(3)/Kair	1σ	Hp(3)/Kair	1σ	Hp(3)/Kair	1σ
degree	Sv/Gy	%	Sv/Gy	%	Sv/Gy	%
0	1.286	0.2	1.240	0.2	1.209	0.2
10	1.288	0.1	1.242	0.1	1.212	0.2
15	1.289	0.1	1.240	0.1	1.212	0.2
20	1.288	0.1	1.241	0.1	1.214	0.2
30	1.289	0.1	1.240	0.1	1.210	0.2
45	1.292	0.1	1.249	0.1	1.223	0.2
60	1.295	0.1	1.254	0.1	1.228	0.2
75	1.270	0.1	1.237	0.1	1.215	0.2
90	1.126	0.1	1.118	0.2	1.112	0.2
105	0.826	0.2	0.850	0.2	0.867	0.2
120	0.583	0.2	0.621	0.2	0.651	0.2
135	0.435	0.2	0.476	0.2	0.510	0.2
150	0.348	0.2	0.392	0.2	0.425	0.3
165	0.304	0.2	0.346	0.3	0.381	0.3
180	0.293	0.3	0.332	0.4	0.366	0.4

Table 7 : $H_p(3)/K_{air}$ conversion coefficient for 600, 700 and 800 keV for different incident angles calculated with PENELOPE in terms of kerma approximation.

Energy (keV)	**600**		**700**		**800**	
Angle	Hp(3)/Kair	1σ	Hp(3)/Kair	1σ	Hp(3)/Kair	1σ
degree	Sv/Gy	%	Sv/Gy	%	Sv/Gy	%
0	1.189	0.2	1.174	0.3	1.167	0.3
10	1.190	0.2	1.173	0.2	1.164	0.2
15	1.192	0.2	1.177	0.2	1.164	0.2
20	1.192	0.2	1.174	0.2	1.167	0.2
30	1.198	0.2	1.174	0.2	1.168	0.2
45	1.202	0.2	1.184	0.2	1.175	0.2
60	1.207	0.2	1.192	0.2	1.181	0.2
75	1.200	0.2	1.188	0.2	1.178	0.2
90	1.104	0.2	1.103	0.2	1.100	0.2
105	0.883	0.2	0.893	0.2	0.901	0.2
120	0.676	0.2	0.699	0.2	0.714	0.2
135	0.541	0.2	0.568	0.2	0.588	0.3
150	0.456	0.3	0.484	0.3	0.507	0.3
165	0.411	0.3	0.439	0.3	0.461	0.3
180	0.397	0.4	0.423	0.4	0.447	0.4

Table 8 : $H_p(3)/K_{air}$ conversion coefficient for 900, 1000 and 1100 keV for different incident angles calculated with PENELOPE in terms of kerma approximation.

Energy (keV)	**900**		**1000**		**1100**	
Angle	Hp(3)/Kair	1σ	Hp(3)/Kair	1σ	Hp(3)/Kair	1σ
degree	Sv/Gy	%	Sv/Gy	%	Sv/Gy	%
0	1.153	0.3	1.152	0.3	1.144	0.3
10	1.156	0.2	1.146	0.2	1.143	0.2
15	1.157	0.2	1.149	0.2	1.141	0.2
20	1.155	0.2	1.156	0.2	1.146	0.2
30	1.159	0.2	1.147	0.2	1.144	0.2
45	1.165	0.2	1.156	0.2	1.154	0.2
60	1.175	0.2	1.162	0.2	1.157	0.2
75	1.171	0.2	1.163	0.2	1.161	0.2
90	1.097	0.2	1.099	0.2	1.098	0.2
105	0.913	0.2	0.915	0.2	0.927	0.2
120	0.734	0.2	0.750	0.3	0.763	0.3
135	0.607	0.3	0.630	0.3	0.639	0.3
150	0.530	0.3	0.549	0.3	0.564	0.3
165	0.485	0.3	0.504	0.3	0.521	0.3
180	0.470	0.4	0.487	0.4	0.509	0.4

Table 9 : $H_p(3)/K_{air}$ conversion coefficient for 1500, 2000 and 3000 keV for different incident angles calculated with PENELOPE in terms of kerma approximation.

Energy (keV)	**1500**		**2000**		**3000**	
Angle	Hp(3)/Kair	1σ	Hp(3)/Kair	1σ	Hp(3)/Kair	1σ
degree	Sv/Gy	%	Sv/Gy	%	Sv/Gy	%
0	1.126	0.3	1.116	0.2	1.110	0.2
10	1.133	0.3	1.115	0.2	1.109	0.2
15	1.129	0.2	1.122	0.2	1.110	0.2
20	1.133	0.3	1.121	0.2	1.111	0.2
30	1.131	0.2	1.121	0.2	1.111	0.2
45	1.140	0.3	1.128	0.2	1.117	0.2
60	1.149	0.2	1.130	0.2	1.117	0.2
75	1.143	0.2	1.128	0.2	1.117	0.2
90	1.093	0.2	1.088	0.2	1.083	0.2
105	0.945	0.3	0.963	0.2	0.977	0.2
120	0.804	0.3	0.836	0.2	0.865	0.2
135	0.696	0.3	0.737	0.2	0.778	0.2
150	0.624	0.3	0.671	0.2	0.718	0.2
165	0.584	0.3	0.632	0.2	0.683	0.2
180	0.571	0.5	0.620	0.3	0.671	0.3

Table 10 : $H_p(3)/K_{air}$ conversion coefficient for 4000, 5000 and 6000 keV for different incident angles calculated with PENELOPE in terms of kerma approximation.

Energy (keV)	**4000**		**5000**		**6000**	
Angle	Hp(3)/Kair	1σ	Hp(3)/Kair	1σ	Hp(3)/Kair	1σ
degree	Sv/Gy	%	Sv/Gy	%	Sv/Gy	%
0	1.103	0.3	1.100	0.3	1.091	0.4
10	1.103	0.2	1.095	0.2	1.088	0.3
15	1.097	0.2	1.095	0.2	1.088	0.3
20	1.101	0.2	1.097	0.2	1.085	0.3
30	1.102	0.2	1.096	0.2	1.089	0.3
45	1.106	0.2	1.097	0.2	1.087	0.3
60	1.104	0.2	1.096	0.2	1.093	0.3
75	1.106	0.2	1.094	0.2	1.084	0.3
90	1.077	0.2	1.068	0.2	1.058	0.3
105	0.990	0.2	0.992	0.2	0.987	0.3
120	0.893	0.2	0.906	0.3	0.913	0.3
135	0.819	0.2	0.838	0.3	0.848	0.3
150	0.766	0.3	0.786	0.3	0.800	0.3
165	0.733	0.3	0.761	0.3	0.770	0.3
180	0.723	0.4	0.749	0.4	0.761	0.4

Table 11 : $H_p(3)/K_{air}$ conversion coefficient for 7000, 8000 and 10000 keV for different incident angles calculated with PENELOPE in terms of kerma approximation.

Energy (keV)	**7000**		**8000**		**10000**	
Angle	Hp(3)/Kair	1s	Hp(3)/Kair	1s	Hp(3)/Kair	1σ
degree	Sv/Gy	%	Sv/Gy	%	Sv/Gy	%
0	1.085	0.4	1.080	0.4	1.072	0.4
10	1.084	0.3	1.080	0.3	1.063	0.3
15	1.084	0.3	1.080	0.3	1.071	0.3
20	1.080	0.3	1.075	0.3	1.072	0.3
30	1.084	0.3	1.078	0.3	1.066	0.3
45	1.082	0.3	1.077	0.3	1.070	0.3
60	1.083	0.3	1.073	0.3	1.071	0.3
75	1.078	0.3	1.072	0.3	1.063	0.3
90	1.051	0.3	1.044	0.3	1.044	0.3
105	0.986	0.3	0.984	0.3	0.975	0.3
120	0.913	0.3	0.913	0.3	0.912	0.3
135	0.852	0.3	0.856	0.3	0.856	0.3
150	0.805	0.3	0.811	0.3	0.821	0.3
165	0.779	0.3	0.789	0.3	0.794	0.3
180	0.775	0.4	0.788	0.4	0.788	0.5

3.3 $H_p(3)/K_{air}$ conversion coefficients, with $H_p(3)$ calculated in terms of absorbed dose

The $H_p(3)/K_{air}$ conversion coefficients have been calculated for thirty energy values from 20 keV up to 10 MeV with the Monte-Carlo code PENELOPE in terms of absorbed dose. The values and the 1 σ type A estimated uncertainties are given in the table 12 to 21.

Table 12 : $H_p(3)/K_{air}$ conversion coefficient for 20, 30 and 40 keV for different incident angles calculated with PENELOPE in terms of absorbed dose.

Energy (keV)	**20**		**30**		**40**	
Angle	**Hp(3)/Kair**	**1σ**	**Hp(3)/Kair**	**1σ**	**Hp(3)/Kair**	**1σ**
degree	**Sv/Gy**	**%**	**Sv/Gy**	**%**	**Sv/Gy**	**%**
0	0.918	0.1	1.221	0.1	1.449	0.2
10	0.915	0.1	1.218	0.1	1.447	0.1
15	0.912	0.1	1.211	0.1	1.444	0.1
20	0.906	0.1	1.211	0.1	1.436	0.1
30	0.890	0.1	1.199	0.1	1.426	0.1
45	0.845	0.1	1.165	0.1	1.390	0.1
60	0.755	0.1	1.096	0.1	1.322	0.1
75	0.562	0.1	0.947	0.1	1.181	0.2
90	0.201	0.1	0.587	0.1	0.846	0.2
105	0.017	0.5	0.195	0.3	0.404	0.2
120	_	_	0.057	0.5	0.181	0.3
135	_	_	0.020	0.8	0.094	0.5
150	_	_	_	_	0.059	0.6
165	_	_	_	_	0.044	0.7
180	_	_	_	_	0.040	1.0

Table 13 : $H_p(3)/K_{air}$ conversion coefficient for 50, 60 and 70 keV for different incident angles calculated with PENELOPE in terms of absorbed dose.

Energy (keV)	**50**		**60**		**70**	
Angle	Hp(3)/Kair	1σ	Hp(3)/Kair	1σ	Hp(3)/Kair	1σ
degree	Sv/Gy	%	Sv/Gy	%	Sv/Gy	%
0.0	1.602	0.2	1.664	0.2	1.670	0.2
10.0	1.595	0.1	1.664	0.1	1.672	0.1
15.0	1.591	0.1	1.661	0.1	1.666	0.1
20.0	1.589	0.1	1.656	0.1	1.665	0.1
30.0	1.572	0.1	1.642	0.1	1.652	0.1
45.0	1.536	0.1	1.607	0.1	1.621	0.1
60.0	1.473	0.1	1.544	0.1	1.568	0.1
75.0	1.333	0.1	1.414	0.2	1.450	0.1
90.0	1.008	0.2	1.107	0.2	1.152	0.1
105.0	0.555	0.2	0.654	0.2	0.703	0.2
120.0	0.296	0.3	0.372	0.3	0.419	0.2
135.0	0.176	0.4	0.237	0.3	0.276	0.3
150.0	0.122	0.4	0.173	0.4	0.205	0.3
165.0	0.099	0.5	0.143	0.4	0.172	0.3
180.0	0.091	0.7	0.134	0.6	0.162	0.5

Table 14 : $H_p(3)/K_{air}$ conversion coefficient for 80, 90 and 100 keV for different incident angles calculated with PENELOPE in terms of absorbed dose.

Energy (keV)	**80**		**90**		**100**	
Angle	Hp(3)/Kair	1σ	Hp(3)/Kair	1σ	Hp(3)/Kair	1σ
degree	Sv/Gy	%	Sv/Gy	%	Sv/Gy	%
0	1.643	0.2	1.612	0.2	1.579	0.2
10	1.646	0.1	1.611	0.1	1.580	0.1
15	1.642	0.1	1.609	0.1	1.579	0.1
20	1.640	0.1	1.608	0.1	1.577	0.1
30	1.630	0.1	1.599	0.1	1.571	0.1
45	1.607	0.1	1.576	0.1	1.553	0.1
60	1.558	0.1	1.535	0.1	1.516	0.1
75	1.446	0.1	1.438	0.1	1.426	0.1
90	1.171	0.1	1.172	0.1	1.174	0.1
105	0.734	0.2	0.748	0.2	0.758	0.2
120	0.444	0.2	0.460	0.2	0.470	0.2
135	0.297	0.3	0.310	0.3	0.321	0.3
150	0.223	0.3	0.236	0.3	0.244	0.3
165	0.190	0.3	0.200	0.3	0.207	0.3
180	0.179	0.5	0.189	0.4	0.196	0.5

Table 15 : $H_p(3)/K_{air}$ conversion coefficient for 110, 150 and 200 keV for different incident angles calculated with PENELOPE in terms of absorbed dose.

Energy (keV)	**110**		**150**		**200**	
Angle	Hp(3)/Kair	1σ	Hp(3)/Kair	1σ	Hp(3)/Kair	1σ
degree	Sv/Gy	%	Sv/Gy	%	Sv/Gy	%
0	1.553	0.2	1.448	0.2	1.374	0.2
10	1.549	0.1	1.447	0.1	1.373	0.2
15	1.549	0.1	1.449	0.1	1.374	0.2
20	1.547	0.1	1.446	0.1	1.374	0.2
30	1.545	0.1	1.444	0.1	1.373	0.2
45	1.530	0.1	1.438	0.1	1.372	0.2
60	1.492	0.1	1.421	0.1	1.368	0.2
75	1.412	0.1	1.360	0.1	1.319	0.2
90	1.167	0.1	1.151	0.2	1.139	0.2
105	0.759	0.2	0.776	0.2	0.796	0.2
120	0.478	0.2	0.503	0.2	0.534	0.3
135	0.329	0.3	0.353	0.3	0.383	0.3
150	0.251	0.3	0.272	0.3	0.299	0.3
165	0.214	0.3	0.234	0.3	0.257	0.4
180	0.201	0.5	0.221	0.5	0.246	0.5

Table 16 : $H_p(3)/K_{air}$ conversion coefficient for 300, 400 and 500 keV for different incident angles calculated with PENELOPE in terms of absorbed dose.

Energy (keV)	**300**		**400**		**500**	
Angle	Hp(3)/Kair	1σ	Hp(3)/Kair	1σ	Hp(3)/Kair	1σ
degree	Sv/Gy	%	Sv/Gy	%	Sv/Gy	%
0	1.284	0.2	1.241	0.3	1.212	0.3
10	1.286	0.2	1.243	0.2	1.210	0.2
15	1.286	0.2	1.243	0.2	1.213	0.2
20	1.285	0.2	1.241	0.2	1.209	0.2
30	1.287	0.2	1.248	0.2	1.215	0.2
45	1.294	0.2	1.250	0.2	1.224	0.2
60	1.293	0.2	1.258	0.2	1.224	0.2
75	1.267	0.2	1.238	0.2	1.214	0.2
90	1.128	0.2	1.120	0.2	1.112	0.2
105	0.828	0.2	0.852	0.2	0.865	0.3
120	0.582	0.2	0.624	0.3	0.653	0.3
135	0.433	0.3	0.477	0.3	0.509	0.3
150	0.350	0.3	0.392	0.3	0.423	0.3
165	0.304	0.3	0.348	0.3	0.381	0.3
180	0.291	0.5	0.328	0.5	0.367	0.5

Table 17 : $H_p(3)/K_{air}$ conversion coefficient for 600, 700 and 800 keV for different incident angles calculated with PENELOPE in terms of absorbed dose.

Energy (keV)	**600**		**700**		**800**	
Angle	Hp(3)/Kair	1σ	Hp(3)/Kair	1σ	Hp(3)/Kair	1σ
degree	Sv/Gy	%	Sv/Gy	%	Sv/Gy	%
0	1.188	0.3	1.179	0.2	1.164	0.3
10	1.188	0.2	1.177	0.2	1.168	0.2
15	1.189	0.2	1.179	0.2	1.164	0.2
20	1.191	0.2	1.180	0.2	1.167	0.2
30	1.196	0.2	1.182	0.2	1.170	0.2
45	1.201	0.2	1.190	0.2	1.178	0.2
60	1.207	0.2	1.194	0.2	1.183	0.2
75	1.197	0.2	1.191	0.2	1.180	0.2
90	1.105	0.2	1.105	0.2	1.105	0.2
105	0.884	0.2	0.895	0.2	0.904	0.3
120	0.677	0.3	0.698	0.2	0.720	0.3
135	0.543	0.3	0.566	0.2	0.586	0.3
150	0.459	0.3	0.484	0.2	0.507	0.3
165	0.414	0.3	0.438	0.2	0.460	0.3
180	0.398	0.5	0.425	0.3	0.448	0.5

Table 18 : $H_p(3)/K_{air}$ conversion coefficient for 900, 1000 and 1100 keV for different incident angles calculated with PENELOPE in terms of absorbed dose.

Energy (keV)	**900**		**1000**		**1100**	
Angle	Hp(3)/Kair	1σ	Hp(3)/Kair	1σ	Hp(3)/Kair	1σ
degree	Sv/Gy	%	Sv/Gy	%	Sv/Gy	%
0	1.160	0.2	1.153	0.3	1.131	0.2
10	1.159	0.2	1.147	0.2	1.129	0.2
15	1.156	0.2	1.152	0.2	1.137	0.2
20	1.158	0.2	1.149	0.2	1.139	0.2
30	1.161	0.2	1.152	0.2	1.144	0.2
45	1.168	0.2	1.158	0.2	1.151	0.2
60	1.174	0.2	1.169	0.2	1.157	0.2
75	1.170	0.2	1.165	0.2	1.159	0.2
90	1.101	0.2	1.102	0.3	1.098	0.2
105	0.911	0.2	0.919	0.3	0.930	0.2
120	0.735	0.2	0.751	0.3	0.760	0.2
135	0.609	0.2	0.627	0.3	0.643	0.2
150	0.529	0.2	0.549	0.3	0.567	0.2
165	0.484	0.2	0.505	0.3	0.521	0.2
180	0.470	0.3	0.489	0.5	0.505	0.3

Table 19 : $H_p(3)/K_{air}$ conversion coefficient for 1500, 2000 and 3000 keV for different incident angles calculated with PENELOPE in terms of absorbed dose.

Energy (keV)	**1500**		**2000**		**3000**	
Angle	Hp(3)/Kair	1σ	Hp(3)/Kair	1σ	Hp(3)/Kair	1σ
degree	Sv/Gy	%	Sv/Gy	%	Sv/Gy	%
0	0.977	0.2	0.742	0.4	0.463	0.4
10	0.982	0.2	0.751	0.2	0.472	0.2
15	0.989	0.2	0.766	0.3	0.482	0.2
20	0.997	0.2	0.781	0.2	0.498	0.2
30	1.021	0.2	0.817	0.3	0.542	0.2
45	1.061	0.2	0.898	0.2	0.646	0.2
60	1.103	0.2	0.985	0.2	0.780	0.2
75	1.126	0.2	1.053	0.2	0.915	0.2
90	1.088	0.2	1.058	0.2	0.986	0.2
105	0.950	0.2	0.954	0.3	0.942	0.2
120	0.805	0.2	0.833	0.3	0.864	0.2
135	0.694	0.2	0.739	0.3	0.786	0.2
150	0.624	0.2	0.675	0.3	0.733	0.2
165	0.583	0.2	0.636	0.3	0.700	0.2
180	0.571	0.3	0.623	0.4	0.689	0.3

Table 20 : $H_p(3)/K_{air}$ conversion coefficient for 4000, 5000 and 6000 keV for different incident angles calculated with PENELOPE in terms of absorbed dose.

Energy (keV)	**4000**		**5000**		**6000**	
Angle	Hp(3)/Kair	1σ	Hp(3)/Kair	1σ	Hp(3)/Kair	1σ
degree	Sv/Gy	%	Sv/Gy	%	Sv/Gy	%
0	0.329	0.5	0.252	0.5	0.201	0.5
10	0.332	0.3	0.256	0.4	0.208	0.4
15	0.341	0.3	0.263	0.4	0.212	0.4
20	0.353	0.3	0.272	0.4	0.221	0.4
30	0.389	0.3	0.303	0.4	0.244	0.4
45	0.487	0.3	0.381	0.3	0.313	0.4
60	0.636	0.3	0.528	0.3	0.444	0.3
75	0.809	0.3	0.723	0.3	0.647	0.3
90	0.927	0.3	0.878	0.3	0.838	0.3
105	0.925	0.2	0.911	0.3	0.892	0.2
120	0.873	0.2	0.871	0.3	0.872	0.2
135	0.813	0.2	0.826	0.3	0.830	0.2
150	0.764	0.2	0.781	0.3	0.792	0.2
165	0.733	0.2	0.756	0.3	0.770	0.2
180	0.724	0.3	0.746	0.4	0.761	0.3

Table 21 : $H_p(3)/K_{air}$ conversion coefficient for 7000, 8000 and 10000 keV for different incident angles calculated with PENELOPE in terms of absorbed dose.

Energy (keV)	**7000**		**8000**		**10000**	
Angle	Hp(3)/Kair	1s	Hp(3)/Kair	1s	Hp(3)/Kair	1σ
degree	Sv/Gy	%	Sv/Gy	%	Sv/Gy	%
0	0.170	0.5	0.147	0.6	0.115	0.6
10	0.175	0.4	0.150	0.4	0.117	0.4
15	0.178	0.4	0.153	0.4	0.120	0.4
20	0.185	0.4	0.158	0.4	0.124	0.4
30	0.204	0.4	0.176	0.4	0.137	0.4
45	0.262	0.4	0.225	0.4	0.176	0.4
60	0.381	0.3	0.332	0.4	0.261	0.4
75	0.589	0.3	0.536	0.3	0.446	0.4
90	0.797	0.3	0.758	0.3	0.699	0.3
105	0.879	0.3	0.864	0.2	0.841	0.3
120	0.864	0.2	0.862	0.2	0.855	0.3
135	0.830	0.2	0.831	0.2	0.831	0.3
150	0.799	0.2	0.800	0.2	0.805	0.3
165	0.773	0.2	0.784	0.2	0.787	0.3
180	0.772	0.3	0.776	0.3	0.781	0.4

4 Discussions

In order to illustrate the discussion, some of the $H_p(3)/K_{air}$ conversion coefficients versus photon energy are represented in the figures 3 to 12 for 0 to 180 degree incident angles. It is to be noted that the errors bars are not visible on the graphs, being hidden by the size of the representative points. The green triangles represent the calculations performed by ENEA with the Monte-Carlo code MCNP [2]. The pink spots represent the values calculated in this work with the Monte-Carlo code PENELOPE [6] with the kerma approximation considering that the energy transferred by the photons to the secondary electrons is deposited at the point of interaction without the simulation of the transport of electrons through the medium. The blue diamond-shaped points represent the values calculated in this work with PENELOPE taking into account the simulation of the electron transport through the medium for the determination of $H_p(3)$, meaning that absorbed dose is determined.

In all conditions, the MCNP values (F6 tally specification card, which correspond to a kerma estimation, must have been used) agree with the values calculated with PENELOPE in the kerma approximation mode.

Nevertheless, above 1 MeV, the discrepancy between kerma approximation and absorbed dose values increase with the photon energy. This difference is drastic at small incident angles and decreases significantly from 90 degree to 180 degree.

This difference at high energy is due to the lack of electronic equilibrium at depths lower than the range of electrons in the medium. As the representative point of the lens is situated at the small depth of 3 mm, this effect is perceptible from 1 MeV, and increases with the photon energy as the electron range enlarges.

For a better understanding of this behavior, calculation have been performed in the ICRU slab phantom (30 cm · 30 cm · 15 cm made of 4-element ICRU tissue). Both Absorbed dose and kerma in tissue have been calculated against the depth for 700 keV, 1 MeV, 1.5 MeV and 5 MeV photon energies at several depth in this phantom. The results are summarized in the figures 13 to 16. At the energy of 700 keV the only noticeable difference occurs at the depth of 1 mm. At 3 mm depth, no difference appears between absorbed dose and kerma. At the energy of 1 MeV, there is a very small difference between absorbed dose and kerma values at the depth of 3 mm. For 1.5 MeV, at the depth of 3 mm, the absorbed dose value is only about 70 % of the kerma value. At the same depth, for 5 MeV, the absorbed dose value correspond only to 20 % of the kerma value. The results and the curves would not be exactly the same in the right cylinder phantom developed for eye-lens dosimetry, but very similar.

Figure 17 shows the $H_p(3)/K_{air}$ conversion coefficients versus the incident angle for selected values of the photon beam energy from 20 keV up to 10 MeV. The calculations with PENELOPE have been performed in terms of absorbed dose. At small angles (<90 degree) and for high energies a large decrease of the dose values can be seen in the graphs due to the lack of electronic equilibrium. For angles greater than about 90 degree, due to the cylindrical geometry, the depth in tissue is enough to ensure the electronic equilibrium, so that the values are higher.

Figure18 shows the $H_p(3)/K_{air}$ conversion coefficients versus the incident angle for selected values of the photon beam energy from 20 keV up to 10 MeV. The calculations with PENELOPE have been performed with the kerma approximation. The shape of the curves are very different from the previous ones in figure 17, there is no more a decrease of the dose values at small angles and for high energies. For angles greater than about 90 degree, due to the cylindrical geometry, the depth in tissue is enough to ensure equivalence between the kerma and the absorbed dose, so that the values are close to those in the figure 17.

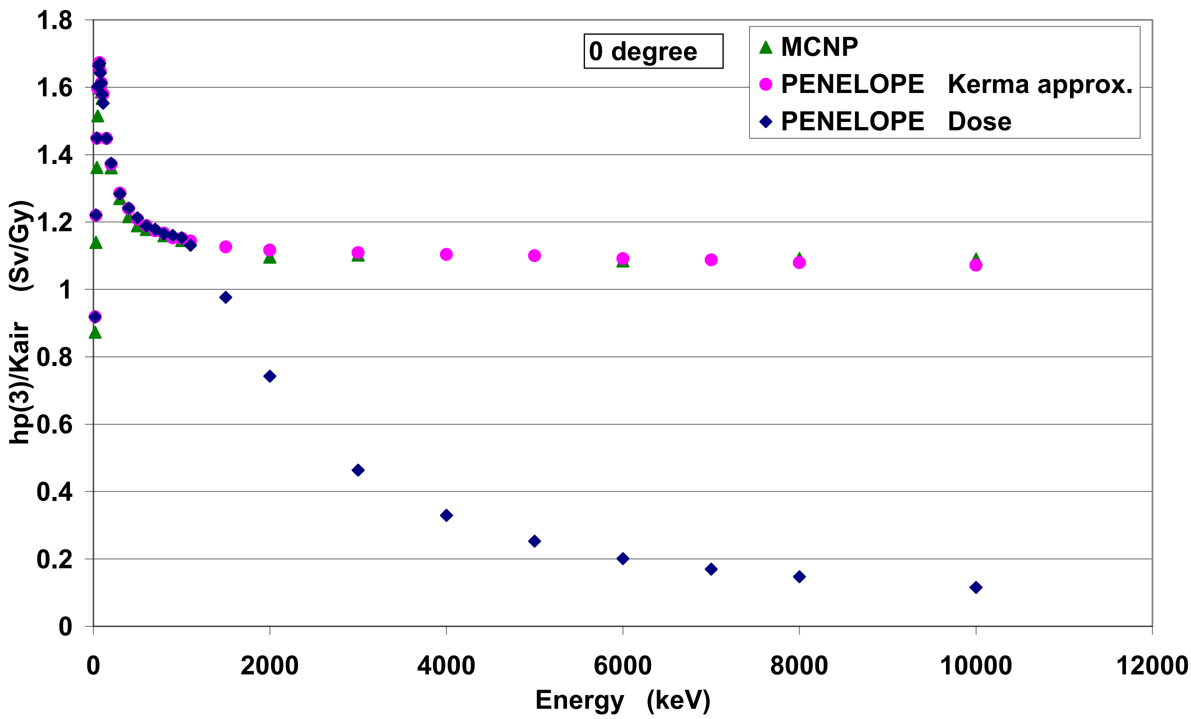

Figure 3 : $H_p(3)/K_{air}$ conversion coefficient versus photon energy at 0 degree incident angle.

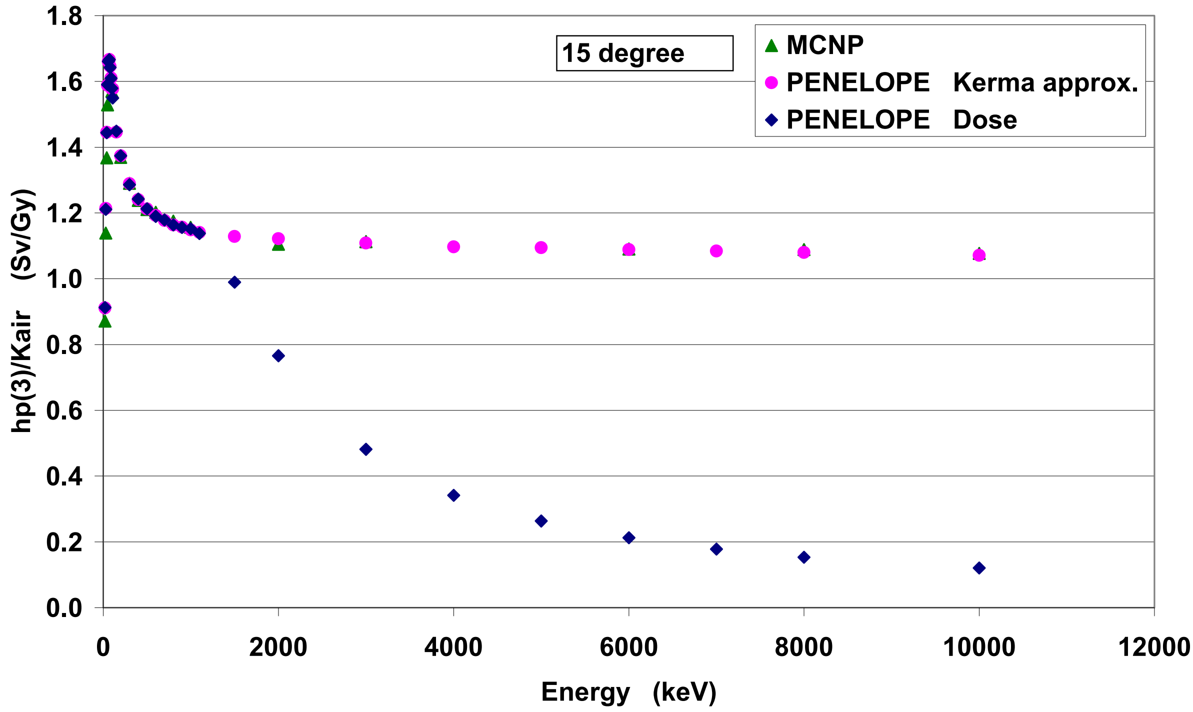

Figure 4 : $H_p(3)/K_{air}$ conversion coefficient versus photon energy at 15 degree incident angle.

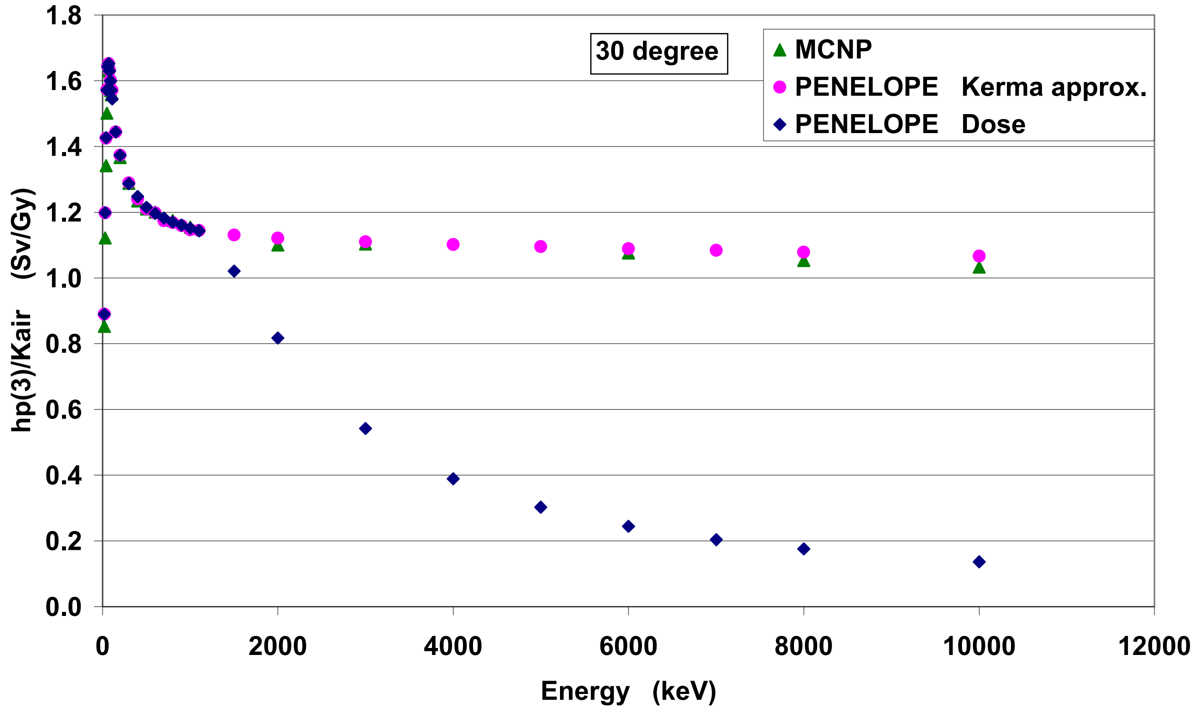

Figure 5 : $H_p(3)/K_{air}$ conversion coefficient versus photon energy at 30 degree incident angle.

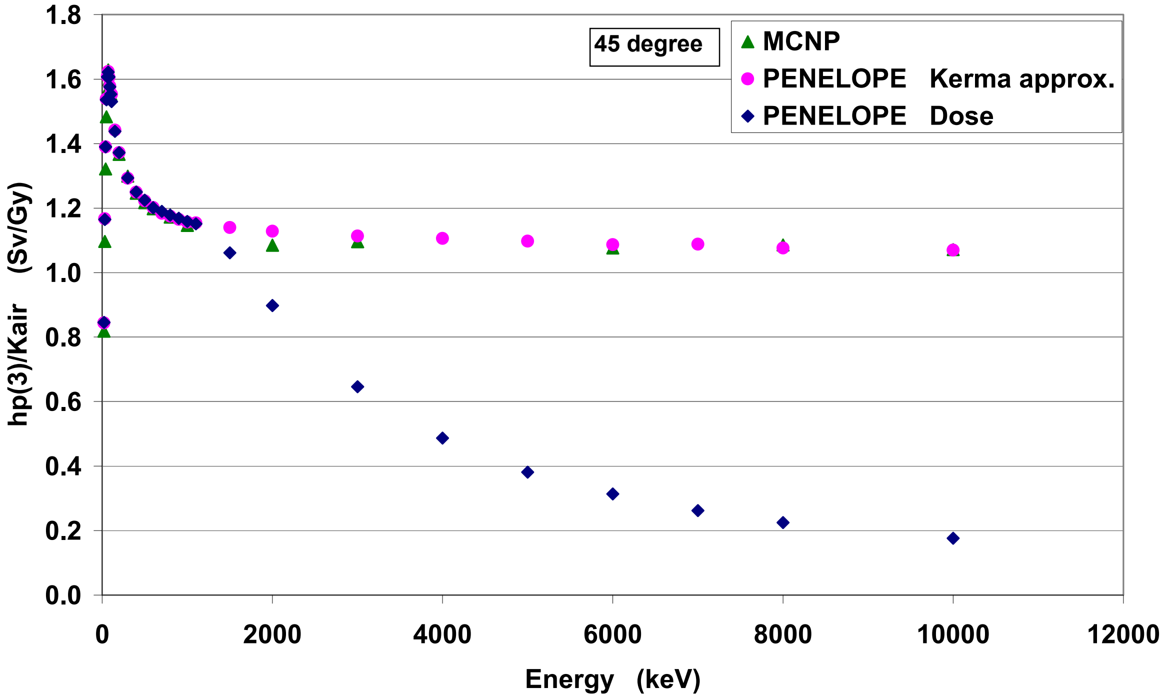

Figure 6 : $H_p(3)/K_{air}$ conversion coefficient versus photon energy at 45 degree incident angle.

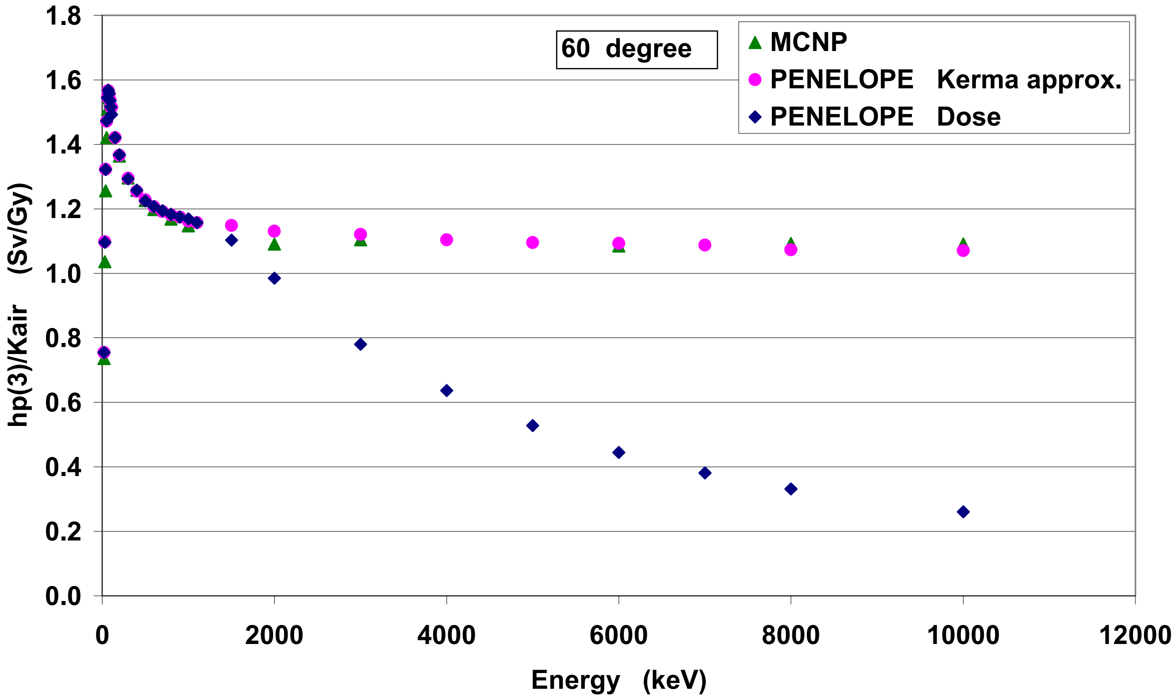

Figure 7 : $H_p(3)/K_{air}$ conversion coefficient versus photon energy at 60 degree incident angle.

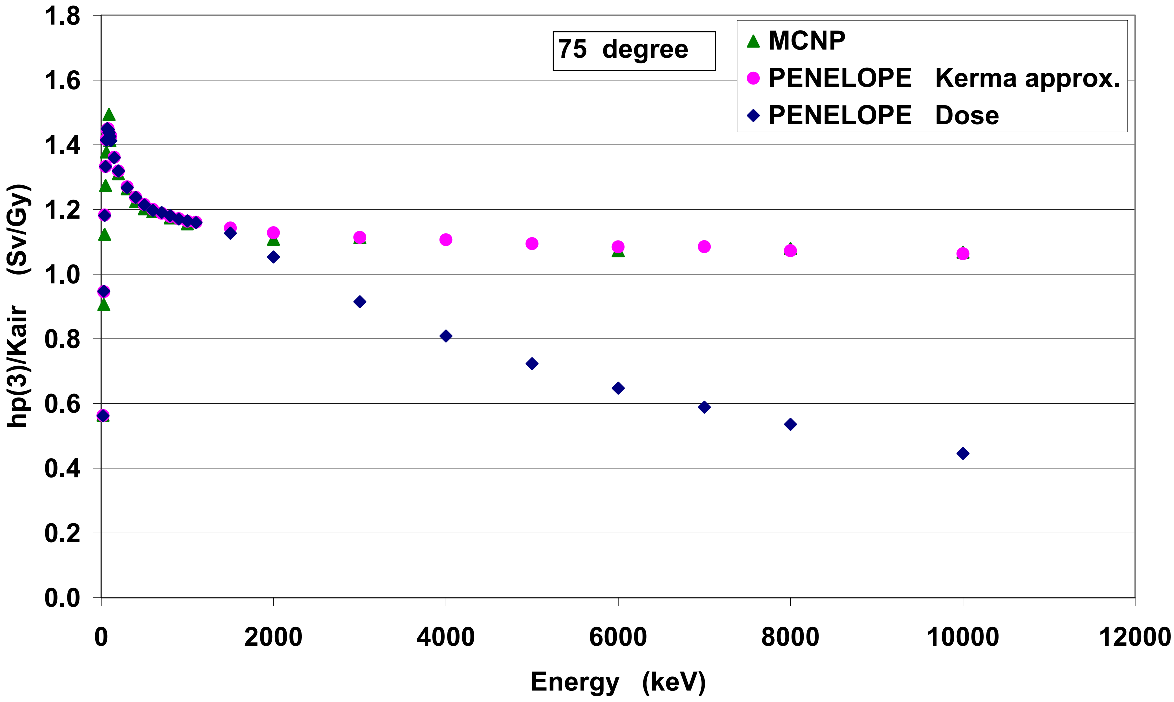

Figure 8 : $H_p(3)/K_{air}$ conversion coefficient versus photon energy at 75 degree incident angle.

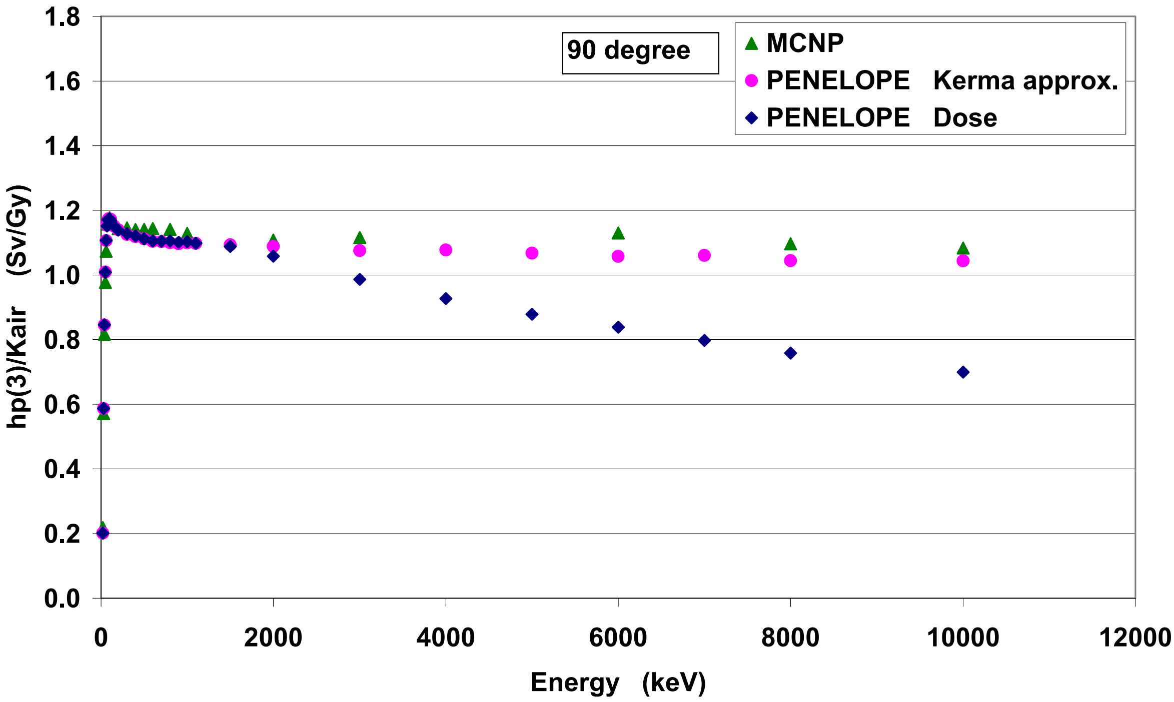

Figure 9 : $H_p(3)/K_{air}$ conversion coefficient versus photon energy at 90 degree incident angle.

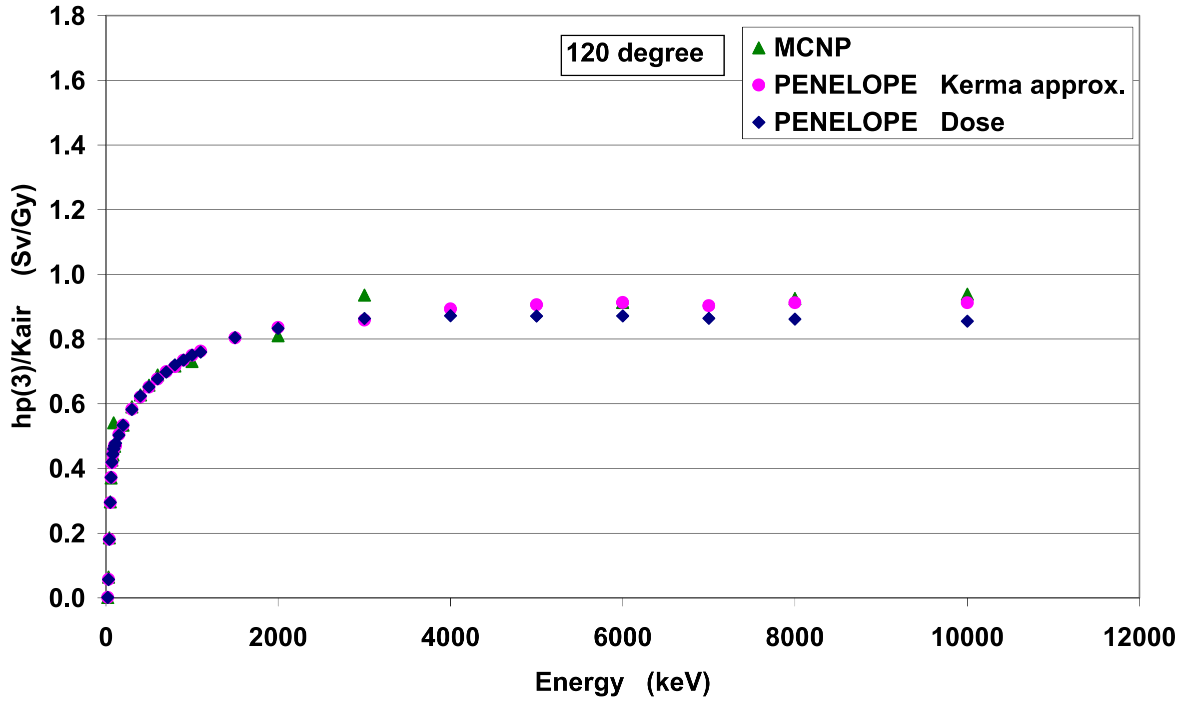

Figure 10 : $H_p(3)/K_{air}$ conversion coefficient versus photon energy at 120 degree incident angle.

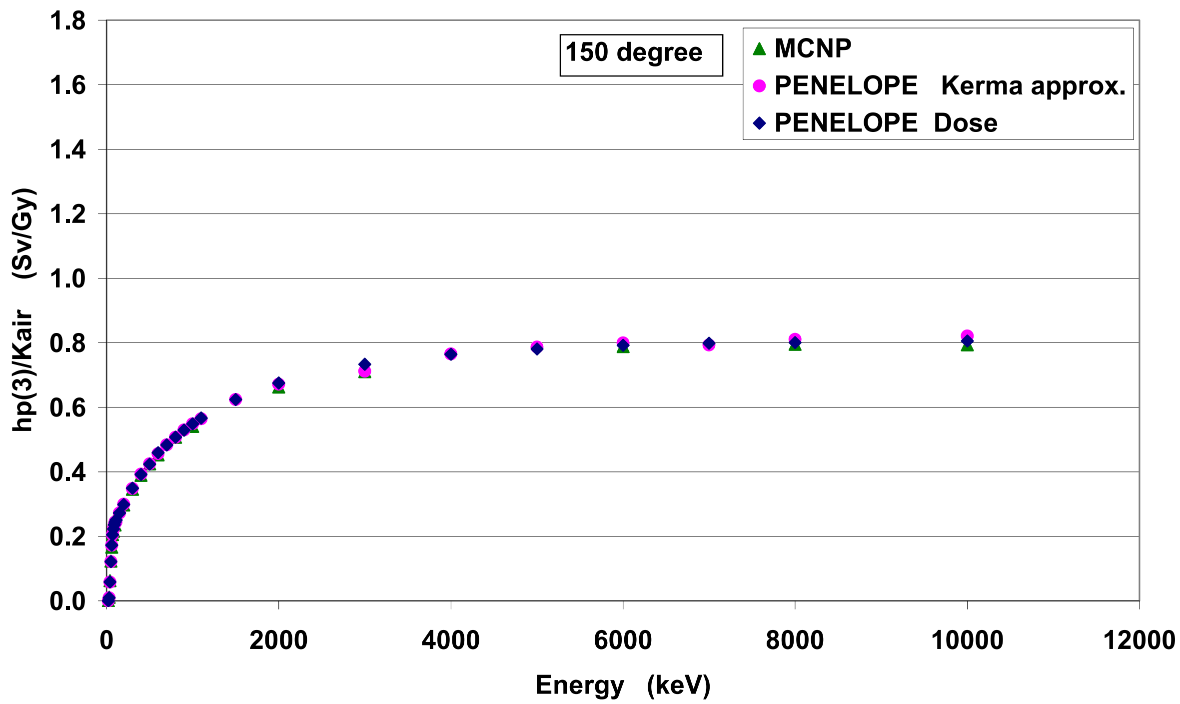

Figure 11 : $H_p(3)/K_{air}$ conversion coefficient versus photon energy at 150 degree incident angle.

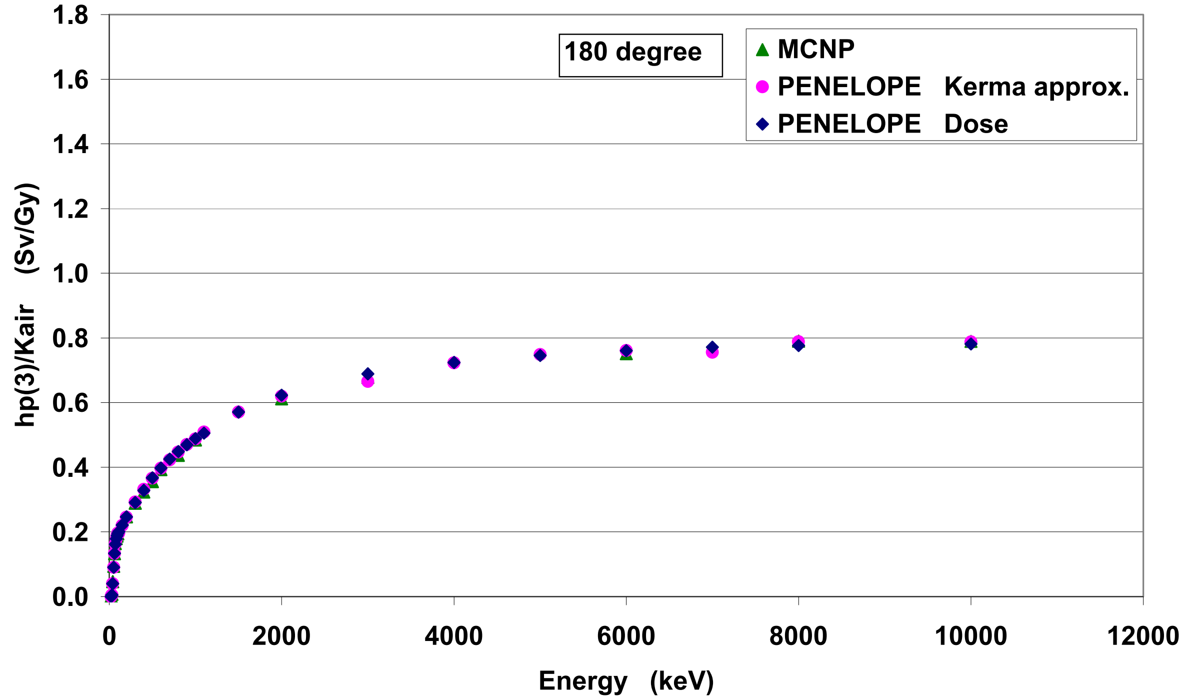

Figure 12 : $H_p(3)/K_{air}$ conversion coefficient versus photon energy at 180 degree incident angle.

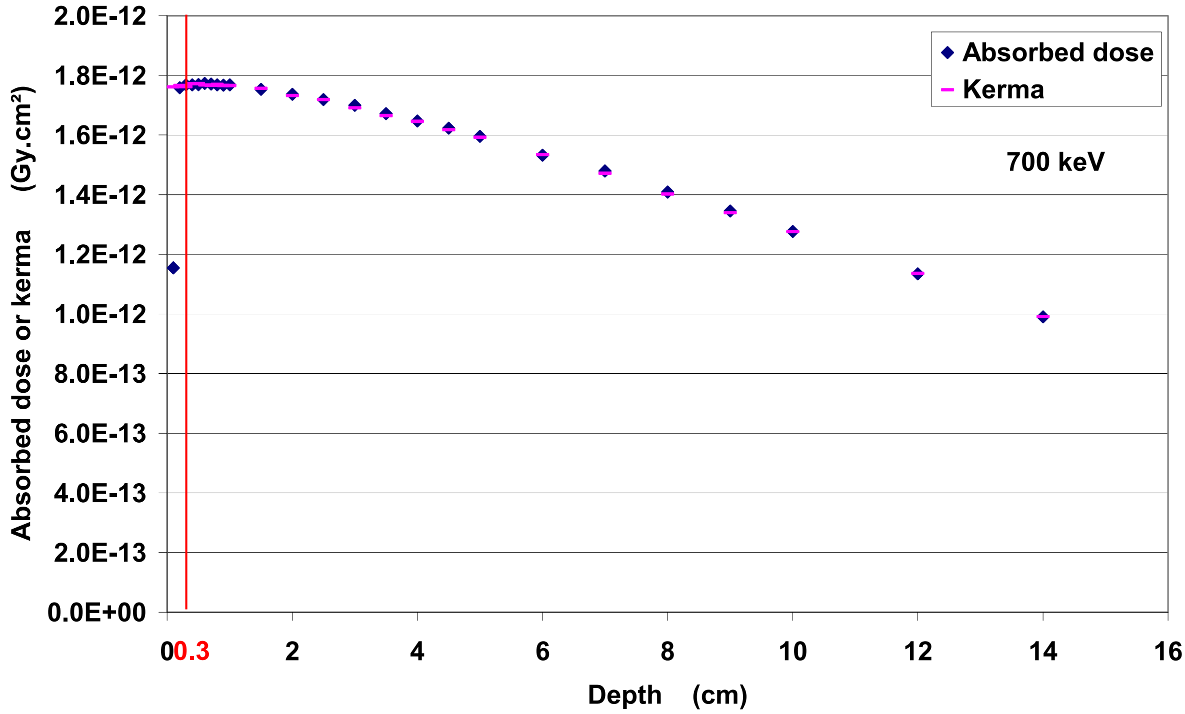

Figure 13: Absorbed dose and kerma in the slab ICRU phantom for 700 keV parallel extended photon beam

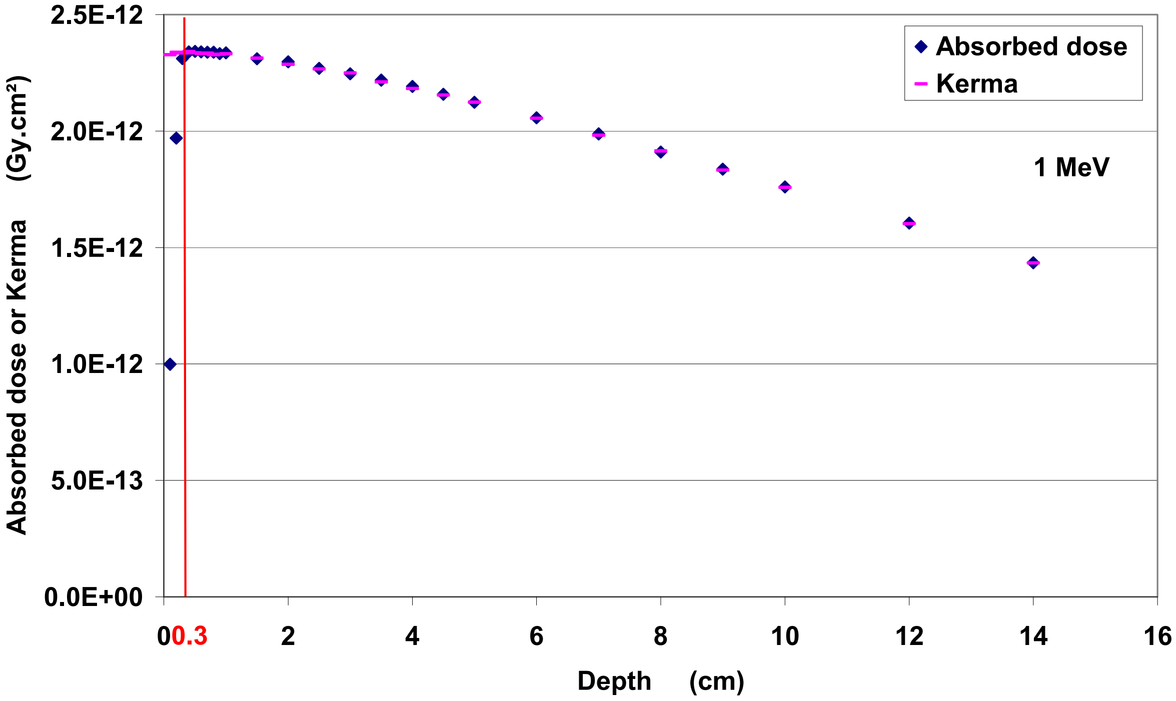

Figure 14: Absorbed dose and kerma in the slab ICRU phantom for 1 MeV parallel extended photon beam

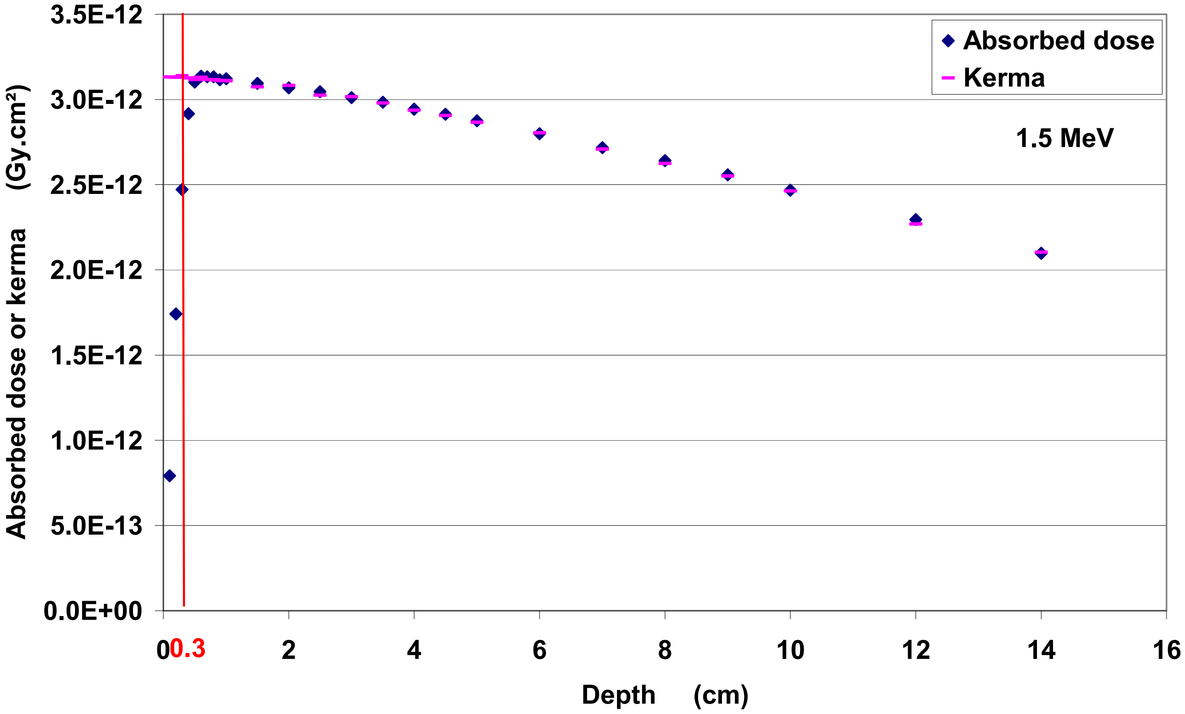

Figure 15: Absorbed dose and kerma in the slab ICRU phantom for 1.5 MeV parallel extended photon beam

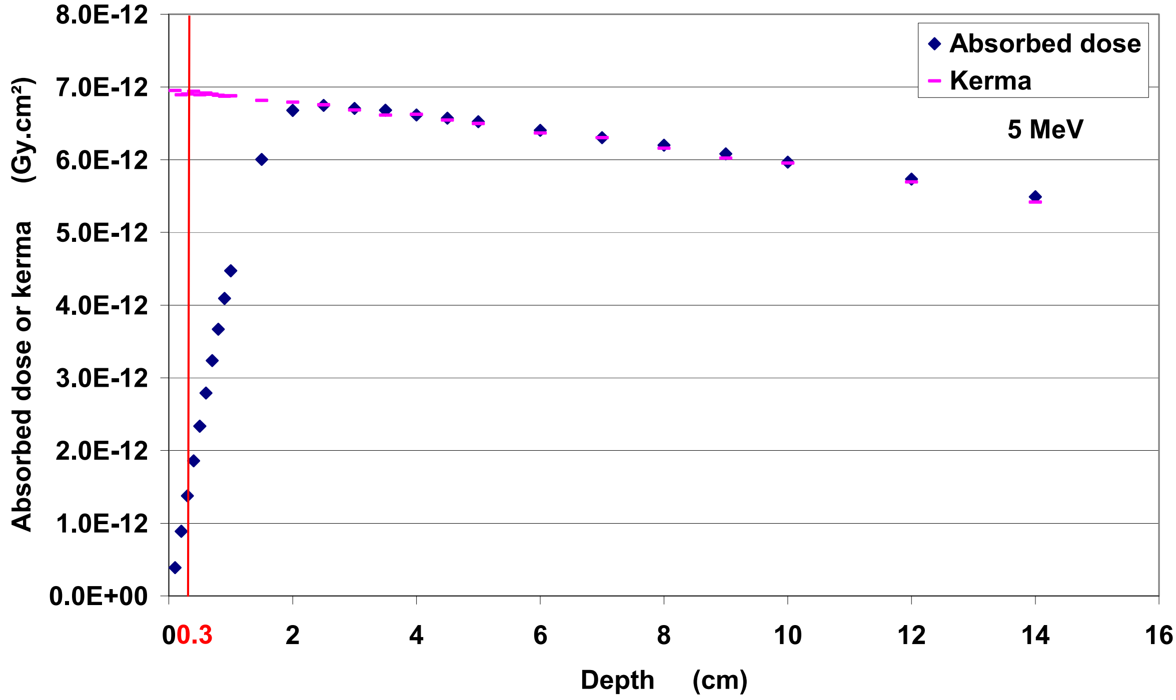

Figure 16: Absorbed dose and kerma in the slab ICRU phantom for 5 MeV parallel extended photon beam

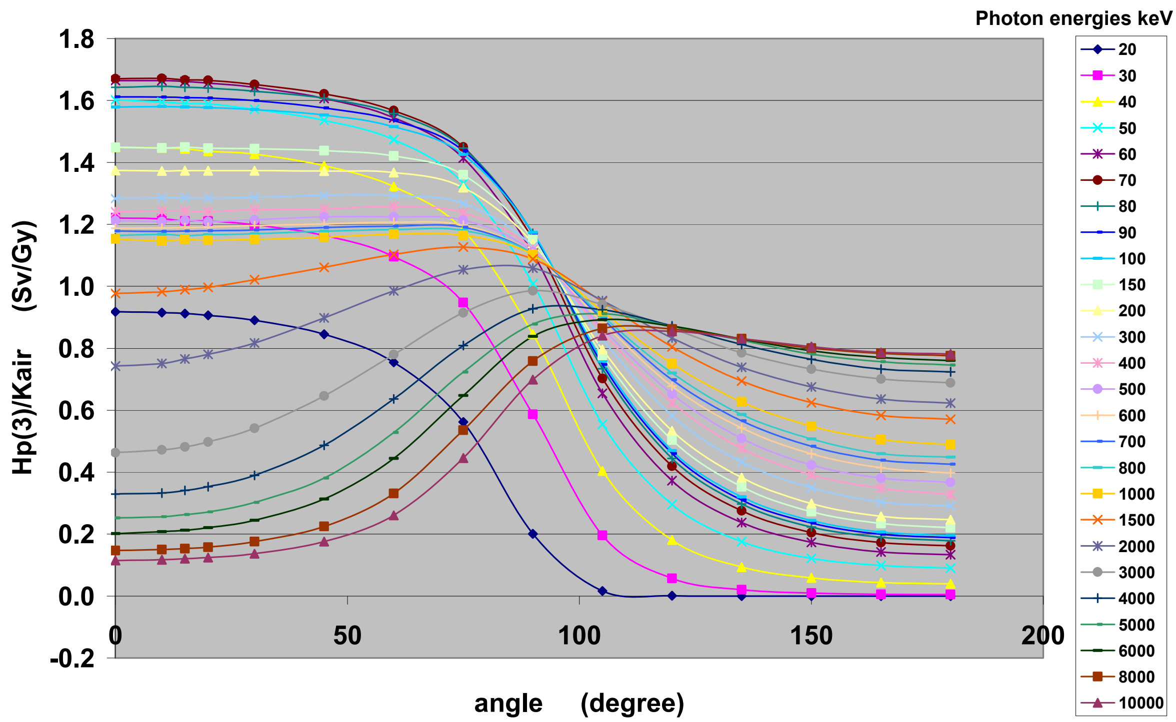

Figure 17: $H_p(3)/K_{air}$ conversion coefficient versus incident angle from 0 to 180 degree calculated in terms of absorbed dose with PENELOPE

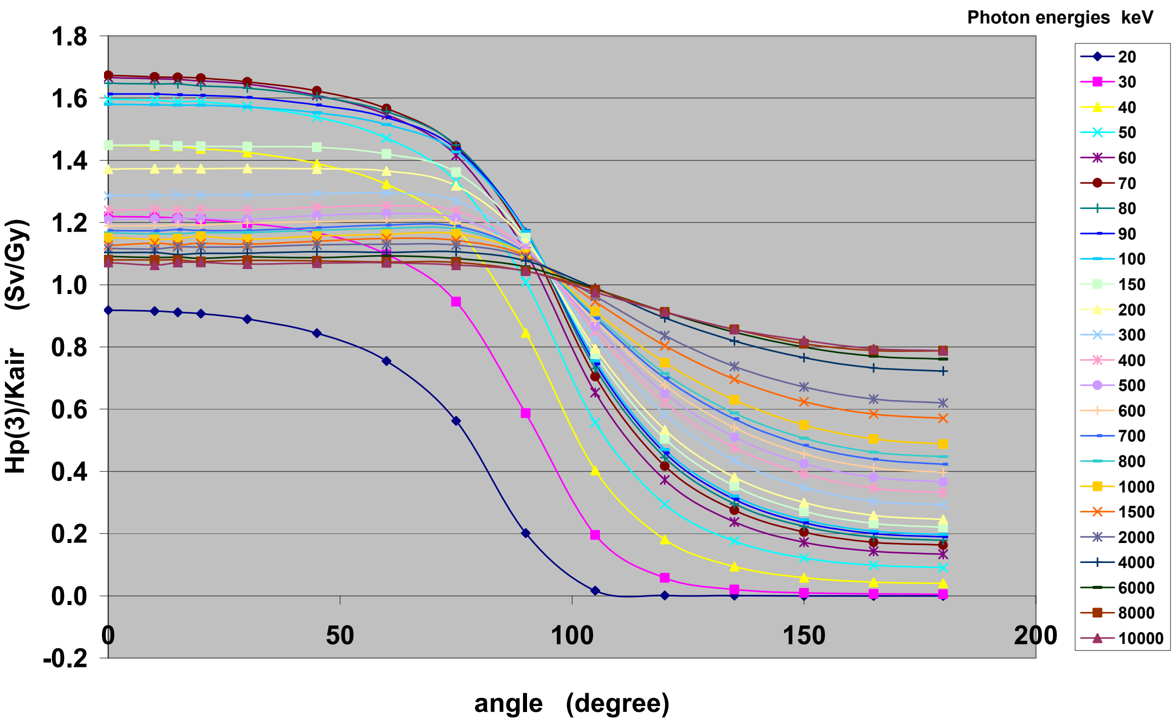

Figure 18: $H_p(3)/K_{air}$ conversion coefficient versus incident angle from 0 to 180 degree calculated with PENELOPE with kerma approximation

5 Conclusions

The $H_p(3)/K_{air}$ conversion coefficients have been determined with the Monte-Carlo code PENELOPE for 30 photon energies from 20 to 10000 keV and for 15 incident angle from 0 to 180 degrees for each photon energy.

The dose equivalent $H_p(3)$ has been determined both in terms of kerma approximation and absorbed dose.

At low photon energy, up to 1 MeV, the two sets of $H_p(3)/K_{air}$ conversion coefficients are consistent. Nevertheless, the differences increase at higher energy. This is mainly due to the lack of electronic equilibrium, especially for small incident angle, lower than 90 degree. Because the computer technology and the Monte-Carlo simulation codes are been improving considerably in recent years, nowadays it is possible to perform the calculation of $H_p(3)$ in terms of absorbed dose instead of kerma approximation.

The values of the conversion coefficients calculated with the Monte-Carlo code MCNP by ENEA [2] are in accordance with the values determined by LNHB with PENELOPE in terms of kerma approximation.

References

[1] ORAMED Contract FP7 Grant Agreement 211361, Bruxelles 2008.

[2] F. Marriotti, G. Gualdrini. ORAMED Project Eye-Lens Dosimetry. A new approach to define the operational quantity $H_p(3)$. ENEA Report RT/2009/1/BAS

[3] ICRU Report 57:1998, Conversion coefficients for use in radiation protection against external radiation.

[4] ICRU Report 47: 1992 Measurement of Dose Equivalents from External Photon and Electron Radiations.

[5] ICRU Report 51: 1993 Quantities and Units in Radiation Protection Dosimetry.

[6] Francesc Salvat, José M. Fernández-Varea and Josep Sempau PENELOPE-2006: A Code System for Monte Carlo Simulation of Electron and Photon Transport

[7] F. TOLA, B. POUMAREDE, B. HABIB, M. GMAR. Optimization of Monte Carlo Codes PENELOPE 2006 and PENFAST by parallelization and variance reduction implementationOPTIMIZATION OF MONTE CARLO CODES PENELOPE 2006 AND PENFAST BY PARALLELIZATION AND REDUCTION VARIANCE IMPLEMENTATION ., Second European Workshop on Monte Carlo Treatment planning. Cardiff 19-21 October MCTP 2009.

[8] G. Dietze and W. G. Alberts Why it is advisable to keep WR=1 and Q=1 for photons and electrons. Radiation Protection Dosimetry (2004), Vol. 109, No. 4, pp. 297-302

[9] ICRP Publication 103. The 2007 Recommendations of the International Commission on Radiological Protection

[10] J.H.Hubbell, S.M.Seltzer : Tables of X-ray mass attenuation coefficients and mass energy-absorption coefficients, NISTIR 5632, Gaithersburg, MD: National Institute of Standards and Technology, 1995.

ÉDITÉ PAR
LA DIRECTION DES SYSTÈMES
D'INFORMATION

CEA / SACLAY 91191 GIF-SUR-YVETTE CEDEX FRANCE